



## Nickel electrowinning using a Pt catalysed hydrogen-diffusion anode. Part II: Batch tank with a sulphate bath

J. RAMBLA<sup>1</sup>, E. BRILLAS<sup>1\*</sup> and J. CASADO<sup>2</sup>

<sup>1</sup>Laboratori de Ciència i Tecnologia Electroquímica de Materials, Departament de Química Física, Facultat de Química, Universitat de Barcelona, Martí i Franquès 1-11, 08028 Barcelona, Spain

<sup>2</sup>Departamento de Investigación, Carburos Metálicos S.A., Pº Zona Franca 14-20, 08038 Barcelona, Spain  
(\*author for correspondence)

Received 3 November 1998; accepted in revised form 27 April 1999

**Key words:** batch tank, electrowinning, hydrogen-diffusion anode, nickel, sulphate bath

### Abstract

A batch tank of 1.6 L capacity has been designed for Ni electrowinning using a Pt catalysed H<sub>2</sub>-diffusion anode and a stainless steel/Ni cathode, both of 100 cm<sup>2</sup> area. The anode has high stability for sulphate baths of pH 3.5 with 35 g L<sup>-1</sup> H<sub>3</sub>BO<sub>3</sub> and Ni<sup>2+</sup> concentrations from 10 g L<sup>-1</sup> up to saturation. Linear correlations between the cell voltage and current intensity are found, as expected for ohmic control of the process. Good electrowinning conditions at room temperature are obtained for Ni<sup>2+</sup> contents from 50 g L<sup>-1</sup>, using an interelectrode gap of 2 cm and regulating the solution pH by NaOH addition for periods of 30 min. Current efficiencies  $\geq 93\%$  are always found. The energy costs increase linearly with increasing current density from 10 to 50 mA cm<sup>-2</sup>, with values much lower than those obtained using a conventional lead anode. This indicates that the Pt catalysed H<sub>2</sub>-diffusion anode is preferable for Ni electrowinning. The crystals are composed of high-purity Ni and have a face-centred cubic structure. Surface analysis by SEM shows that the grain size gradually increases with increasing current density, with no significant influence of the Ni<sup>2+</sup> concentration.

### 1. Introduction

Electrowinning from baths containing NiCl<sub>2</sub> and/or NiSO<sub>4</sub> in the presence of high concentrations of H<sub>3</sub>BO<sub>3</sub> are used for the production of high-purity nickel [1–3]. Several factors, such as electrolysis conditions and electrolyte composition, affect the grain size, orientation, structure and surface morphology of the recovered nickel crystals [4–7]. The main disadvantages of the method arise from the use of conventional DSA, graphite or lead anodes, which yield deposits slightly contaminated with inorganic impurities, such as lead, iron, cobalt, copper and sulfur, along with high energy consumption due to the overvoltage required for the oxidation of water to oxygen at the anode.

A notable improvement in the process has been reported [8, 9] when an alternative H<sub>2</sub>-diffusion anode with a stable catalyst able to oxidize hydrogen to protons is used. The energy cost decreases significantly due to the much lower energy consumed for hydrogen oxidation at this anode compared to water oxidation in conventional anodes. The H<sub>2</sub>-diffusion anode also allows high-purity nickel to be obtained because possible deposit contamination due to corrosion is avoided. However, the production of protons during batch electrolysis causes an increase in bath acidity, thus

hindering the formation of adherent deposits. This problem must be solved by pH regulation within the optimum pH range 2–4 for long-time electrolysis [8]. In previous work [9], the behaviour of a small 100 mL cell containing a Pt catalysed H<sub>2</sub>-diffusion anode of area 3.1 cm<sup>2</sup> was studied using typical chloride, Watts and sulphate baths for Ni electrowinning. Evolution of chlorine gas at the anode was detected with the chloride bath. The existence of this competitive anodic reaction suggests that Watts and sulphate media will be better for use of the proposed anode in industrial cells.

This paper describes a study of nickel electrowinning carried out in a batch tank of 1.6 L capacity, designed to operate with a Pt catalysed H<sub>2</sub>-diffusion anode and a stainless steel/nickel cathode, both of 100 cm<sup>2</sup> area, under similar conditions as reported previously for a small three-electrode cell [9]. Since the anode loses performance in the presence of chloride ions, the study has been restricted to a sulphate bath. The electrochemical characteristics of the reactor at different interelectrode gaps have been investigated to find its best operating conditions. The effects of Ni<sup>2+</sup> concentration and current density on the current efficiency and energy cost have been considered. The purity, crystallographic orientation and surface morphology of the deposits have also been determined.

## 2. Experimental details

The composition and preparation of the chloride bath, as well as the instruments employed for SEM, EDS and XRD analysis of nickel deposits, have been reported in previous work [9]. Sulphate baths with different  $\text{Ni}^{2+}$  concentrations and the Watts medium were prepared with  $\text{NiSO}_4 \cdot 6 \text{H}_2\text{O}$  of analytical grade supplied by Merck. All these baths contained  $35 \text{ g L}^{-1} \text{ H}_3\text{BO}_3$  and their initial pH value was about 3.5. The other chemicals used were analytical reagents from Merck and Probus.

Figure 1 shows a scheme of the batch tank designed to use a Pt catalysed  $\text{H}_2$ -diffusion anode (denoted as carbon-PTFE [Pt] anode) for nickel electrowinning. The cell of  $10 \text{ cm} \times 15 \text{ cm} \times 18 \text{ cm}$  in dimension was constructed with polytetrafluoroethylene (PTFE)-coated steel to avoid the acidic attack. The anode had  $12 \text{ cm} \times 12 \text{ cm} \times 0.5 \text{ mm}$  in dimension and was supplied by E-TEK. It was composed of a carbon cloth with both sides coated with about  $5 \text{ mg cm}^{-2}$  of carbon black Vulcan XC-72 + PTFE with 10 wt % Pt. The anode was in contact with a stainless steel frame as electrical connection, which was coupled to the feed chamber. This pack was pressed onto a face of the cell, centred to a square hole of  $100 \text{ cm}^2$  area. The anode became operative when pure hydrogen gas at a constant rate, regulated by a flowmeter from Cole-Parmer, was supplied to the feed chamber. The base material of the cathode was a polished stainless steel plate of  $10 \text{ cm} \times 12 \text{ cm} \times 0.1 \text{ cm}$  in dimension. It was suspended into the cell by a copper wire as electrical connection, parallel to the anode, with its opposite side covered with an inert polymer to avoid its coating. Further, 1.6 L of the  $\text{Ni}^{2+}$  bath tested were introduced into the cell and the apparent area of this plate was limited to  $100 \text{ cm}^2$ . The stainless steel/nickel cathode was prepared by pre-electrolysing the bath at 1 A for 5 min at room temperature ( $23 \pm 2 \text{ }^\circ\text{C}$ ). A fresh bath and a new cathode were used for each trial.

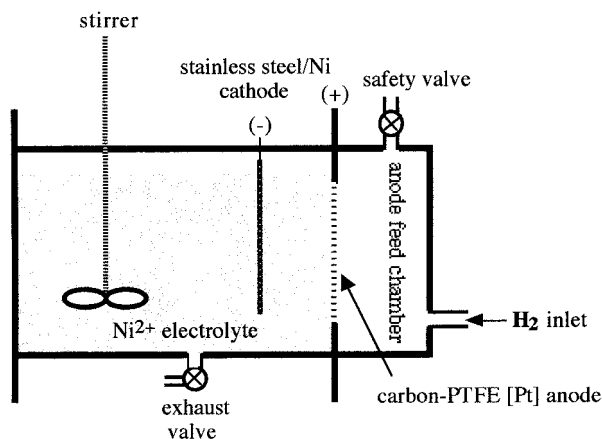


Fig. 1. Scheme of the batch tank used for nickel electrowinning. The apparent area of both electrodes in contact with the  $\text{Ni}^{2+}$  electrolyte was  $100 \text{ cm}^2$  and the bath volume was 1.6 L.

All electrochemical experiments were performed by applying a constant current density,  $j$ , for 3 h at room temperature using an Amel 555A potentiostat-galvanostat connected to an Amel 721 current integrator. The cell voltage,  $V$ , was measured using a Demestres 605 digital multimeter. In some cases, the electrolyte bulk was mechanically stirred by means of a PTFE-coated steel shaft coupled to a Schott RM144 stirrer. The deposit was detached from the cathode, rinsed with water and dried by air to constant weight. The current efficiency and energy cost were calculated from the weight of recovered nickel.

## 3. Results and discussion

### 3.1. Stability of the Pt catalysed $\text{H}_2$ -diffusion anode in chloride and Watts baths

The first trials on nickel electrowinning were performed with a chloride bath of  $300 \text{ g L}^{-1} \text{ NiCl}_2 \cdot 6 \text{ H}_2\text{O} + 35 \text{ g L}^{-1} \text{ H}_3\text{BO}_3$ , which is the medium giving the lowest cell voltages and energy costs in the three-electrode cell studied previously [9]. However, the anode was unstable and high cell voltages were found, even with small interelectrode gaps. For example, at  $25 \text{ mA cm}^{-2}$  with an interelectrode gap of 2 cm,  $V$  increased from 3.8 to 4.4 V for 25 min and the experiment was stopped due to the production of large amounts of chlorine at the anode by the fast oxidation of chloride ions. This phenomenon can not be prevented even supplying hydrogen gas to the anode at a rate at least double the value predicted for its overall oxidation to protons. The existence of this competitive anodic reaction explains the malfunction of the anode in the chloride bath. The behaviour of a Watts medium with low chloride content, where an insignificant rate for the anodic oxidation of this anion is expected [9], was then studied.

Electrolysis at  $10 \text{ mA cm}^{-2}$  with an interelectrode gap of 1.5 cm was carried out for a Watts bath of  $300 \text{ g L}^{-1} \text{ NiSO}_4 \cdot 7 \text{ H}_2\text{O} + 45.5 \text{ g L}^{-1} \text{ NiCl}_2 \cdot 6 \text{ H}_2\text{O} + 35 \text{ g L}^{-1} \text{ H}_3\text{BO}_3$ . No chloride evolution at the anode was observed, but after 3 h, only 64% current efficiency was obtained, while the energy cost was as high as  $2.7 \text{ kW h kg}^{-1}$ . These results are much inferior to those obtained in a three-electrode cell under potentiostatic conditions [9]. This may be associated with the higher cell voltage (close to 1.9 V) in the batch tank, along with a bigger decay in solution pH, which varies from 3.6 to a final value of 1.4. Both effects favour hydrogen evolution instead of nickel electrodeposition.

Several attempts were then made to electrolyse the Watts bath in the optimum pH interval 2–4 [8, 9]. These conditions were achieved at  $10 \text{ mA cm}^{-2}$  by addition of NaOH up to an initial pH  $\sim 4$  or in the presence of a dihydrogenphosphate/phosphoric acid buffer. After 3 h, no reproducible results were obtained for these electrolyses, since efficiencies between 62% and 94% and energy costs from 1.8 to  $2.2 \text{ kW h kg}^{-1}$  were found.

After these trials, the electrocatalyst ability of the anode for oxidizing  $H_2$  was lost. A possible explanation of this effect may be the gradual poisoning and/or blocking of the Pt catalyst by strongly adsorbed chloride ions and/or chlorine atoms formed by slow oxidation. A similar degradation of a  $H_2$ -diffusion anode catalysed by tungsten carbide in the presence of chloride ions has been reported by Nikolova et al. [10].

The above results indicate a loss in performance of the Pt catalysed  $H_2$ -diffusion anode in the batch tank if the electrolyte contains chloride ions. Efforts were then concentrated to show that Ni can be efficiently recovered from sulphate baths. All experiments under these conditions were made with the same anode, with no apparent loss of electroactivity for oxidation of  $H_2$ .

### 3.2. Electrochemical behaviour of the plant with sulphate baths

Before studying the nickel electrowinning from sulphate baths, the  $V/j$  curves of the system with  $Ni^{2+}$  concentrations between 10 and 125  $g\ L^{-1}$  (saturated solution) were determined to establish the best conditions for long-duration electrolyses. These measurements were carried out between 2 and 50  $mA\ cm^{-2}$ . To be sure that the anode was fed with the necessary amount of  $H_2$ , a pure gas flow at least twice higher than the stoichiometric requirement for complete oxidation was supplied for each  $j$  considered.

The change of cell voltage with current density at interelectrode gaps between 1 and 6 cm using a bath with 74  $g\ L^{-1}$   $Ni^{2+}$  (332  $g\ L^{-1}$   $NiSO_4 \cdot 6\ H_2O$ ) + 35  $g\ L^{-1}$   $H_3BO_3$  of pH 3.5 is displayed in Figure 2. At a given interelectrode gap, a linear correlation between  $V$  and  $j$  is always observed from about 1 V, as expected for ohmic control of the overall process. For each  $j$  value, the cell voltage increases with increasing interelectrode gap. This trend can be explained by the progressive increase in resistance to the passage of current. Figure 2 also shows that almost the same  $V/j$

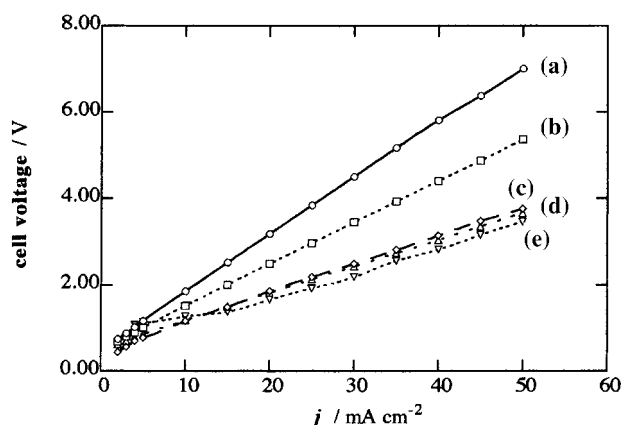


Fig. 2. Variation of cell voltage with current density for nickel electrowinning in the batch tank with a sulphate bath of pH 3.5 containing 35  $g\ L^{-1}$   $H_3BO_3$  and 74  $g\ L^{-1}$   $Ni^{2+}$  at room temperature. Interelectrode gap: (a) 6, (b) 4, (c) and (d) 2 and (e) 1 cm. In curve (c), the electrolyte was stirred at 150 rpm.

curves are obtained under solution stirring (curve (c)) and for a quiescent bath (curve (d)). These results confirm that the process is not limited by the transport of  $H_2$  to the anode and/or  $Ni^{2+}$  towards the cathode, being controlled by the electrolyte resistance (ohmic control), as stated above. Similar curves to those reported in Figure 2 are found for sulphate baths with  $Ni^{2+}$  concentrations between 50 and 125  $g\ L^{-1}$ . In contrast, when the  $Ni^{2+}$  content decreases from 50 to 10  $g\ L^{-1}$ , a gradual increase in cell voltage at a given  $j$  occurs. This behaviour is not related to a loss in electroactivity of the anode for lower  $Ni^{2+}$  concentrations than 50  $g\ L^{-1}$ , since reproducible  $V/j$  plots are always obtained.

### 3.3. Nickel electrowinning from a sulphate bath

All electrolyses for sulphate baths were comparatively performed with an interelectrode gap of 2 cm without solution stirring. This distance was chosen for two reasons: (i) it allows low cell voltages, practically the same values as those of a gap of 1 cm (see Figure 2(d) and 2(e)), thus yielding the minimum energy cost; (ii) the system is stable because reduced  $Ni^{2+}$  ions can be renewed by diffusion from the bulk. The electrolyte was not stirred, since the performance of the system is not improved, as seen by comparison of Figure 2(c) and 2(d).

A simple procedure was applied to regulate the pH of each sulphate bath within 2.0 and 4.0 during electrolysis. The experiment was stopped every 30 min and solid NaOH was added to the solution to re-adjust its pH to about 4. A certain amount of  $Ni(OH)_2$  precipitate was formed, this being completely dissolved under stirring for at least 5 min. Adherent, uniform and compact deposits were obtained using this method.

#### 3.3.1. Effect of $Ni^{2+}$ concentration and current density

Sulphate baths of pH  $\sim 3.5$  with a  $Ni^{2+}$  concentration between 10 and 125  $g\ L^{-1}$  were electrolysed at 10, 20, 30, 40 and 50  $mA\ cm^{-2}$  for 3 h. This is the maximum time expected for the overall nickel consumption (0.273 mol) of 1.6 L of the 10  $g\ L^{-1}$   $Ni^{2+}$  solution at 50  $mA\ cm^{-2}$  assuming 100% current efficiency. Study of this bath allows evaluation of the system for Ni recovery from very low  $Ni^{2+}$  concentrations. In each electrolysis, an oscillating value of  $V$  was found, decreasing with time with progressive pH decay and returning to its initial value when the pH was readjusted to about 4.0 every 30 min.

Figure 3 shows the variation of average cell voltage with initial  $Ni^{2+}$  concentration at 30  $mA\ cm^{-2}$ . The average cell voltage decreases rapidly from 3.73 to 2.01 V when the  $Ni^{2+}$  content increases from 10 to 50  $g\ L^{-1}$ . In contrast, at higher  $Ni^{2+}$  concentrations, it remains almost constant between 1.8 and 1.9 V. The same behaviour is found for all current densities. This trend is similar to that reported above for the  $V/j$  curves of the initial baths and can be better explained taking

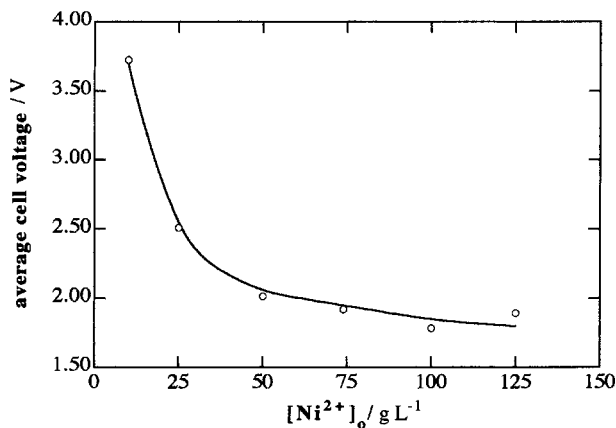


Fig. 3. Dependence of average cell voltage on initial  $\text{Ni}^{2+}$  concentration for nickel electrowinning in the batch tank at an interelectrode gap of 2 cm. Each initial sulphate bath was prepared with  $35 \text{ g L}^{-1} \text{ H}_3\text{BO}_3$  and a current density of  $30 \text{ mA cm}^{-2}$  was applied for 3 h at room temperature. Solution pH adjusted to  $\sim 4.0$  by addition of NaOH each 30 min.

into account the current efficiencies given in Figure 4. While good efficiencies between 92% and 97% are found for  $\text{Ni}^{2+}$  contents between 25 and  $125 \text{ g L}^{-1}$ , it decreases to 73% for  $10 \text{ g L}^{-1} \text{ Ni}^{2+}$ . Under these last conditions, adherent nickel deposits are formed, but  $\text{H}_2$  evolution is observed at the cathode, suggesting that about 27% of current is consumed in reducing protons instead  $\text{Ni}^{2+}$ . For higher  $\text{Ni}^{2+}$  contents, no  $\text{H}_2$  evolution is detected due to the slower rate for proton reduction, corresponding to less than 8% current efficiency. The fact that the cell voltage increases as  $\text{Ni}^{2+}$  concentration decreases from  $50 \text{ g L}^{-1}$  can be mainly ascribed to the increase in solution resistance due the presence of a lower concentration of ions. For  $\text{Ni}^{2+}$  contents  $\leq 10 \text{ g L}^{-1}$ , the cell voltage is sufficiently high to accelerate the parallel  $\text{H}_2$  evolution, thus decreasing the nickel deposition rate. This competitive process could give a higher polarization of the cathode, even increasing  $V$ .

The above results indicate that the Ni recovery from sulphate baths with  $\text{Ni}^{2+}$  contents  $\leq 10 \text{ g L}^{-1}$  using a Pt

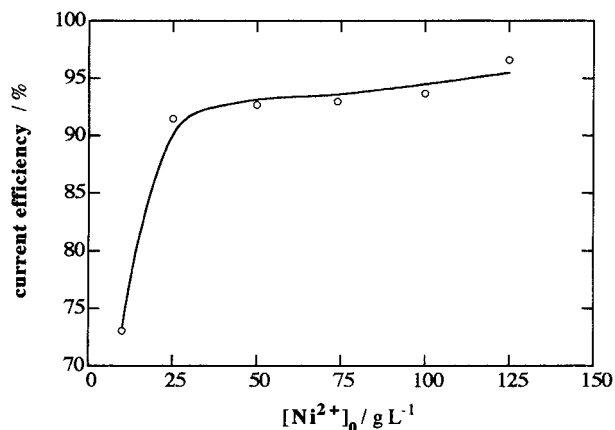


Fig. 4. Current efficiency vs. initial  $\text{Ni}^{2+}$  concentration for the experiments shown in Figure 3.

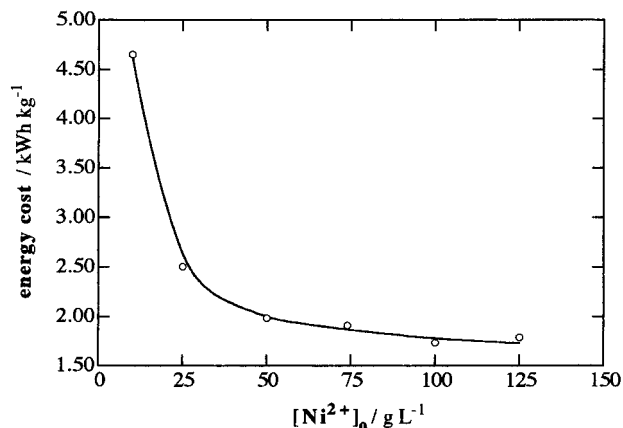


Fig. 5. Variation of energy cost with initial  $\text{Ni}^{2+}$  concentration for the experiments given in Figure 3.

catalysed  $\text{H}_2$ -diffusion anode is an inefficient process. High cell voltages, low current efficiencies and parallel proton reduction are involved in it. In addition, the consumption is very high, close to  $4.5 \text{ kW h kg}^{-1}$  at  $30 \text{ mA cm}^{-2}$ , as shown in Figure 5. The lowest cell voltages with good efficiencies are achieved between 50 and  $125 \text{ g L}^{-1} \text{ Ni}^{2+}$  (Figures 3 and 4). Under these conditions, Figure 5 shows a minimum cost about  $1.8 \text{ kW h kg}^{-1}$  at  $30 \text{ mA cm}^{-2}$ .

High efficiencies between 96% and 98% for the saturated solution and between 93% and 97% for  $74 \text{ g L}^{-1} \text{ Ni}^{2+}$  were obtained for all  $j$  values. The effect of current density on consumption for these electrolytes is presented comparatively in Figure 6. A linear increase in energy cost with increasing current density is observed for each bath. The slightly lower consumption for the saturated solution from  $30 \text{ mA cm}^{-2}$  is mainly due to its lower ohmic resistance which yields a lower cell voltage. At  $50 \text{ mA cm}^{-2}$ , the cost for this bath is  $2.4 \text{ kW h kg}^{-1}$ , indicating that the Pt catalysed  $\text{H}_2$ -diffusion anode can be used in industrial cells under these conditions. Note

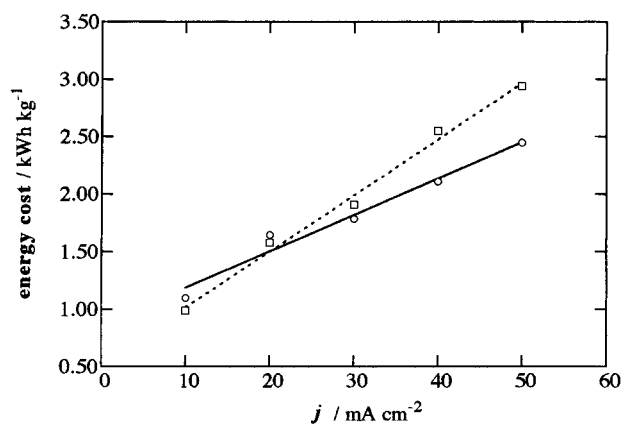


Fig. 6. Change of energy cost with applied current density for nickel electrowinning in the batch tank at an interelectrode gap of 2 cm. The initial sulphate baths were prepared with  $35 \text{ g L}^{-1}$  of  $\text{H}_3\text{BO}_3$  and a  $\text{Ni}^{2+}$  concentration of: (a,  $\circ$ )  $125 \text{ g L}^{-1}$ ; (b,  $\square$ )  $74 \text{ g L}^{-1}$ . All electrolyses were carried out for 3 h at room temperature, and each 30 min NaOH was added to the bath to adjust its pH to  $\sim 4.0$ .

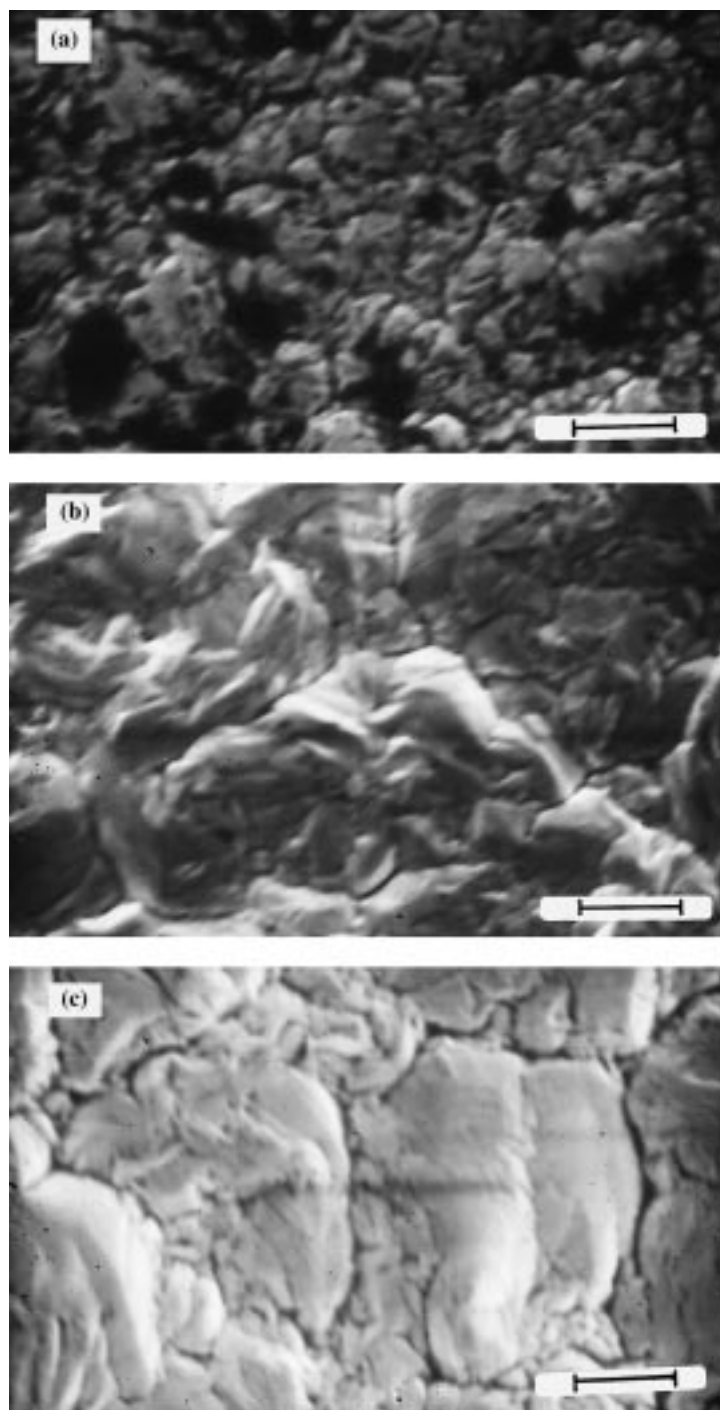


Fig. 7. SEM micrographs for nickel deposits obtained after 3 h of electrolysis of a sulphate bath initially containing  $74 \text{ g L}^{-1} \text{ Ni}^{2+}$ . Applied current density: (a) 10, (b) 30 and (c)  $50 \text{ mA cm}^{-2}$ . Scalebar:  $5 \mu\text{m}$ .

that all energy costs reported in Figure 6 are significantly lower than  $4.3 \text{ kW h kg}^{-1}$  reported for a conventional lead anode in a sulphate bath at  $40 \text{ mA cm}^{-2}$  and at  $60 \text{ }^\circ\text{C}$  [5].

### 3.3.2. Analysis of nickel deposits

The purity of all deposits was checked by EDS. These spectra showed the presence of the L,  $K_\alpha$  and  $K_\beta$  bands of Ni, without signals related to impurities from the anode and the electrolyte. These results confirm the high stability of Pt at the  $\text{H}_2$ -diffusion anode.

XRD spectra recorded for the different deposits showed five peaks, as maximum, associated with the (1 1 1), (2 0 0), (2 2 0), (3 1 1) and (2 2 2) crystallographic planes of nickel. This peak distribution indicates that the crystals have a face-centred cubic lattice. This structure for Ni deposited from sulphate baths has been previously reported by Küceki [5] and by us using a small two-electrode cell [9].

The relative peak intensities of the crystallographic orientations formed from several media are collected in Table 1. The preferential mode of Ni growth is the

Table 1. Relative intensities found by XRD for the crystallographic orientations of Ni deposits obtained after 3 h of electrolysis of a sulphate bath in the batch tank at several current densities and different initial Ni<sup>2+</sup> concentrations

[Ni <sup>2+</sup> ] <sub>0</sub> /g L <sup>-1</sup> j/mA cm <sup>-2</sup>		Crystallographic orientation				
		(1 1 1)	(2 0 0)	(2 2 0)	(3 1 1)	(2 2 2)
25	30	1.1	1.2	100	4.0	0.0
74	10	15	36	100	27	0.0
	30	1.4	2.8	100	6.3	0.0
	50	1.2	2.4	100	5.4	0.0
125*	10	30	100	26	19	2.1
	30	1.2	1.8	100	5.0	0.0
	50	11	2.6	100	9.1	1.0

\* Saturated solution

(2 2 0) plane in all cases, except for the saturated solution, where the (2 0 0) orientation predominates at 10 mA cm<sup>-2</sup>. The deposits from this last bath show other discrepancies. Thus, a weak signal for the (2 2 2) plane is only detected for the saturated solution. In addition, results of Table 1 show a progressive enhancement of the preferential (2 2 0) orientation with increasing *j* for 74 g L<sup>-1</sup> Ni<sup>2+</sup>, whereas for the saturated solution, the minority peaks become more intense when *j* increases from 30 to 50 mA cm<sup>-2</sup>.

The surface morphology of all deposits was examined by SEM. Figure 7(a), (b) and (c) show micrographs for the nickel obtained from 74 g L<sup>-1</sup> Ni<sup>2+</sup> at 10, 30 and 50 mA cm<sup>-2</sup>, respectively. An increase in grain size and higher compactness is observed with increasing current density. The same morphological characteristics are found for all sulphate baths.

#### 4. Conclusions

This work demonstrates that a Pt catalysed H<sub>2</sub>-diffusion anode of 100 cm<sup>2</sup> area can be efficiently used for nickel electrowinning from a sulphate bath in a batch tank of 1.6 L with a stainless steel/nickel cathode of the same area. When a chloride bath was electrolysed, chlorine evolution at the anode competes with H<sub>2</sub> oxidation. The use of a Watts bath gives low current efficiencies, high energy consumptions and a loss in electroactivity of the anode. In contrast, high anode stability and reproducible results are found for sulphate baths of pH ~3.5 with a Ni<sup>2+</sup> concentration higher than 10 g L<sup>-1</sup>. The cell voltage increases with increasing current density and

interelectrode gap, but it does not vary significantly if the solution is stirred. The overall process gives ohmic control at high *j* values.

Electrolyses of sulphate baths were performed at *j* values between 10 and 50 mA cm<sup>-2</sup> for 3 h, at an interelectrode gap of 2 cm, and regulating the pH to ~4.0 by addition of solid NaOH for periods of 30 min. At 10 g L<sup>-1</sup> Ni<sup>2+</sup>, the high H<sub>2</sub>-evolution rate at the cathode caused low current efficiencies. For Ni<sup>2+</sup> contents between 50 and 125 g L<sup>-1</sup>, current efficiencies above 93% and a linear increase in energy cost with *j* were found. The costs were much lower than those obtained for a conventional lead anode. This indicates that the Pt catalysed H<sub>2</sub>-diffusion anode favours the nickel electrowinning process at this scale, confirming the previous results for smaller cells [9]. All deposits were composed of high-purity nickel which crystallizes in a face-centred cubic structure with a preferential (2 2 0) orientation. The surface morphology of deposits did not vary with the Ni<sup>2+</sup> bath content, although the grain size increased progressively with increasing *j*.

#### Acknowledgements

The authors are grateful to Carbueros Metálicos SA for financial support received for this work.

#### References

1. D.J. Mackinnon, 'The Electrowinning of Metals from Aqueous Chloride', in K. Osseo-Asare and J.D. Miller (eds), 'Conference Proceedings of the Metallurgical Society of AIME', Hydrometallurgy Research, Development and Plant Practice, New York (1982), p. 659.
2. E. Jackson, 'Hydrometallurgical Extraction and Reclamation' (Horwood, Chichester, 1986), p. 221.
3. Ullmann's, 'Encyclopedia of Industrial Chemistry', (5th edn), Vol. A17 (VCH, Weinheim, 1994), p. 189.
4. A. Chiba, K. Kitamura and T. Ogawa, *Surf. Coat. Technol.* **27** (1986) 83.
5. E. Küzeci, R. Kammel and S.K. Gogia, *J. Appl. Electrochem.* **24** (1994) 730.
6. J. Ji, W.C. Cooper, D.B. Dreisinger and E. Peters, *J. Appl. Electrochem.* **25** (1995) 642.
7. R.A. Tacken and L. J.J. Janssen, *J. Appl. Electrochem.* **25** (1995) 1.
8. V. Nikolova, T. Nikolov, T. Vitanov, A. Möbius, K. Wiesener and D. Schab, *J. Appl. Electrochem.* **21** (1991) 313.
9. E. Brillas, J. Rambla and J. Casado, *J. Appl. Electrochem.*, Part I of this paper.
10. V. Nikolova, I. Nikolov, V. Titanov and K. Wiesener, *J. Appl. Electrochem.* **23** (1993) 1268.